1.1.4 PIONEER 10 OBSERVATIONS OF ZODIACAL LIGHT BRIGHTNESS NEAR THE ECLIPTIC: CHANGES WITH HELIOCENTRIC DISTANCE

M. S. HANNER, J. G. SPARROW*, J. L. WEINBERG, AND D. E. BEESON
Space Astronomy Laboratory, State University of New York at Albany

Abstract. Sky maps made by the Pioneer 10 Imaging Photopolarimeter (IPP) at sun-spacecraft distances from 1 to 3 AU have been analyzed to derive the brightness of the zodiacal light near the ecliptic at elongations greater than 90 degrees. The change in zodiacal light brightness with heliocentric distance is compared with models of the spatial distribution of the dust. Use of background starlight brightnesses derived from IPP measurements beyond the asteroid belt, where the zodiacal light is not detected, and, especially, use of a corrected calibration lead to considerably lower values for zodiacal light than those reported by us previously.

Introduction. The Pioneer 10/11 zodiacal light experiment has provided the first opportunity to measure the zodiacal light from heliocentric distances greater than 1 AU. It is now complemented by the Helios zodiacal light experiment, which is observing the zodiacal light from positions between 0.3 and 1 AU. The imaging photopolarimeter (IPP) used for zodiacal light observations from Pioneers 10 and 11 is described by Pellicori, et al. (1973). In the sky mapping or zodiacal light mode (Weinberg et al., 1973), orthogonal brightness components are recorded in blue and red bandpasses (half-power wavelengths from 3950A to 4850A and 5900A to 6900A, respectively) as the IPP scans the sky with a 2.3 by 2.3 degree field of view.

Observations from a single heliocentric distance do not yield the particle spatial distribution directly, since the spatial distribution is multiplied by the unknown scattering function of the particles in the integration along the line of sight. While observations from a space probe still require integration along the line of sight, the change in zodiacal light brightness with heliocentric distance of the probe provides information on the large-scale spatial distribution of the dust (Hanner and Leinert, 1972).

The Pioneer 10/11 experiment has the additional advantage that the background starlight component can be observed directly from positions beyond the asteroid belt where the zodiacal light can no longer be seen with the IPP (Weinberg, et al., 1974). This background starlight is then subtracted from the total observed brightness to obtain the brightness of the zodiacal light. The method used to reduce Pioneer 10 brightness observations is described by Weinberg, et al.

---

*On leave from Aeronautical Research Laboratories, Melbourne, Victoria, Australia.

(1974) and was used to derive the zodiacal light brightness in the asteroid belt by Hanner, et al. (1974). In the present paper we extend that analysis by deriving the near-ecliptic zodiacal light brightnesses in the blue for Pioneer 10 distances from 1 to 2.4 AU.

Calibration. An empirical method was used with a number of stars to establish the relation between a star's blue (B) magnitude and the equivalent brightness it contributes over the IPP blue band (Weinberg, et al. 1974). The zero magnitude star calibration was converted to the response to Vega (B magnitude +0.04) and the absolute calibration was based on the flux of Vega (Hayes and Latham 1975) corrected for the effect of H_β, H_γ, and H_δ and integrated over the IPP blue bandpass. The conversion to $S_{10}(V)$* is based on Johnson's (1954) solar spectral irradiance integrated over the IPP blue bandpass and a solar visual magnitude of -26.73 (Stebbins and Kron, 1957). Details of the star calibration and the reasons for changing from the previously used diffuse source calibration are discussed by Weinberg, et al. (in preparation). if the Labs and Neckel (1970) solar irradiance is used, the brightnesses in $S_{10}(V)$ will be raised by 10% for the IPP blue band-pass. To correct for changes in instrument sensitivity, a relative calibration was derived for each sky map using star brightnesses.

The brightnesses given in earlier publications were based on a preflight absolute calibration of the IPP using a C^{14} diffuse source. Due to uncertainties in the absolute radiance of the C^{14} source and in the change of IPP sensitivity between laboratory calibration and flight, we believe the calibration using Vega to be more accurate (Weinberg, et al., in preparation). We estimate our final calibration accuracy to be ±8%, with the largest uncertainty in the effective field of view area. In the course of reanalyzing the calibration data, we also discovered a numerical error of a factor of 2 such that our previously published values are significantly too high:

1. Hanner and Weinberg, 1973. The Gegenschein brightnesses should be multiplied by 0.53. The relative brightness decrease between 1.01 and 1.25 AU remains approximately $1/R^2$. See discussion of Gegenschein in next section.

2. Hanner and Weinberg, 1974. The brightness levels and heliocentric dependence in that preliminary report are superceded by the results given in the present paper.

3. Weinberg, et al., 1974. The background starlight brightnesses should be multiplied by 0.57. This correction decreases the brightnesses in each of the reduction steps illustrated in Figure 3 and the brightness contour levels shown in Figure 4 of that paper.

4. Hanner, et al., 1974. The brightnesses should be multiplied by 0.57. The relative change in brightness with heliocentric distance is not affected.

Observations and Analysis. Data along the ecliptic at elongations $\epsilon > 90$ degrees were analyzed for 15 sky maps between 1.01 and 2.41 AU, following the method described by Weinberg, et. al. (1974) and Hanner, et al. (1974). The data presented here are restricted to the segment

*Equivalent number of 10th magnitude (V) stars of solar spectral type per square degree.

along the ecliptic between ecliptic longitudes $\lambda = 177$ and 230 degrees, where we have derived a composite of the background starlight from sky maps beyond the asteroid belt.

Representative data are shown in Figure 1 for two sky maps, Day 75/1972 and Day 104/1972. The upper data are brightnesses after subtraction of resolved stars but before subtraction of the background starlight. The lower plots show the zodiacal light component after subtraction

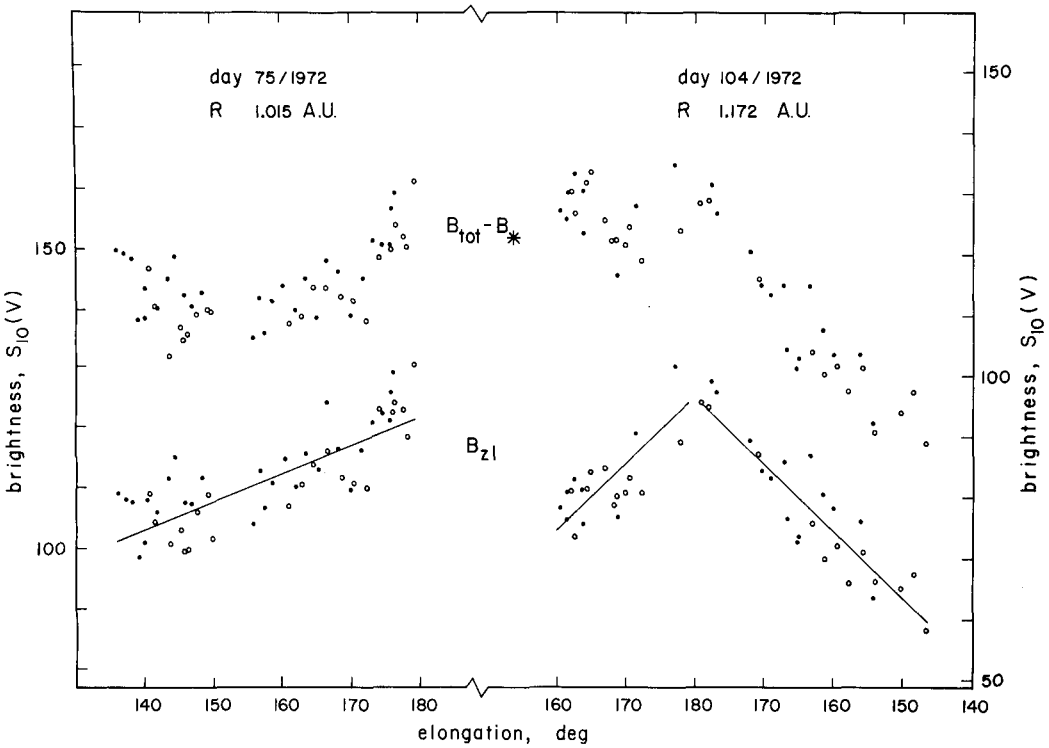

Fig. 1. Observed brightness vs. elongation in the blue spectral band. Filled circles are for $\beta > 0°$, open circles for $\beta < 0°$.

of the background starlight. Both Day 75 and 104 represent observations along the same section of the ecliptic. The lines represent least-squares linear fits to the data for the purpose of intercomparing the brightness versus elongation data from different maps and are not intended to fit the non-linear rise near the Gegenschein.

Although the spacecraft was still near 1 AU on Day 75, it was already 1.5×10^6 km below the ecliptic plane and 5.5×10^6 km below the invariant plane. Theoretical models of the zodiacal light brightness which would be observed from a spacecraft at 1.015 AU and 2 degrees below the plane of symmetry of the dust indicate that a brightness decrease of approximately 10 per cent compared to that observed at 1.00 AU in the symmetry plane can be expected.

It should be pointed out that the direction ϵ = 180 degrees does not lie in the plane of symmetry of the dust distribution, or at ecliptic latitude β = 0 degrees, for a spacecraft position outside the plane of symmetry. As a result, the shape of the brightness distribution near ϵ = 180 degrees is dependent on the off-ecliptic dust distribution as well as on the shape of the particle phase function. With the IPP scanning pattern and field of view we do not have measurements centered at exactly 180 degrees. Furthermore, since the effective field of view is elongated along the direction perpendicular to the ecliptic plane, any sharply peaked function will be smoothed out in our data numbers.

Figure 2 shows schematically the change with elongation and the level of the zodiacal light

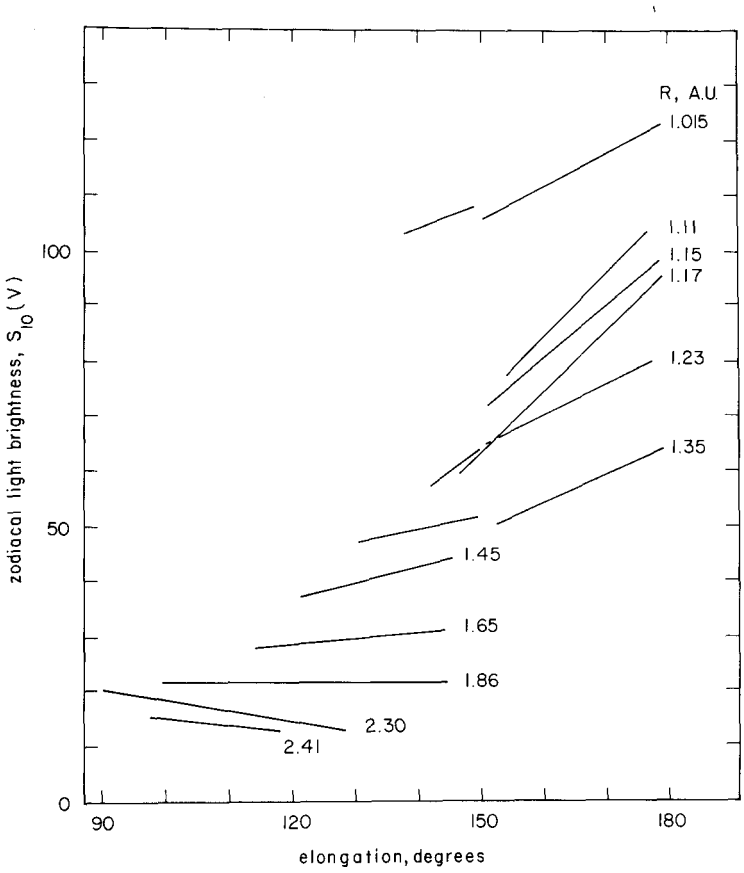

Fig. 2. Smoothed, linear-fit zodiacal light brightnesses in the blue spectral band. R = sun-spacecraft distance in A. U.

brightness for each of the sky maps. The lines represent a least-squares fit to the data, as illustrated in Figure 1. The line at R = 1.015 AU is the average for 5 sky maps made during the first ten days of the mission. The slope from ϵ = 150 to 180 degrees is less steep near 1.015 AU than at R = 1.11 to 1.17 AU. The slopes at R = 1.23 and 1.35 AU are intermediate. We find

no obvious reason for the difference in slopes, which is evident in the total brightness as well as in the zodiacal light component (see Figure 1). Since the same region of sky was scanned in all cases, the same resolved stars and background starlight were subtracted. Between R = 1.015 and 1.35 AU the position of the Gegenschein (ϵ = 180 degrees) as seen from the spacecraft moved from $\lambda = 177^{\circ}$, $\beta = -0.5^{\circ}$ to $\lambda = 228.6^{\circ}$, $\beta = -1.9^{\circ}$, with the result that the brightness plots at R = 1.015 and 1.35 AU are mirror images of each other in ϵ. At R = 1.11 to 1.17 AU, ϵ = 180 degrees was near the center of the plot and the slopes from ϵ = 150 to 180 degrees were identical for the two sides of the plot. Preliminary analysis of Pioneer 10 red data shows a slope on days 75 and 104 which is midway between the corresponding slopes in the blue. Pioneer 11 data will be similarly analyzed.

Radial Dependence. The zodiacal light brightnesses at $130^{\circ} \leq \epsilon \leq 145^{\circ}$ were averaged for each sky map in order to derive the brightness variation with heliocentric distance. Figure 3 shows the averages, compared to the predicted brightness for various models of the dust distribution. 5 to 10 points are included in the averages, and the error bars represent the standard error of the mean at each solar distance. Points shown at heliocentric distances beyond 2.4 AU are data from Hanner, et al. (1974), corrected. As discussed in Hanner, et al. (1974), there is a drop in the zodiacal light brightness between 2.9 and 3.3 AU, indicating an abrupt decrease in the dust particle concentration near 3.3 AU. Beyond 3.3 AU no zodiacal light was detected at $\epsilon > 90$ degrees.

Models of the zodiacal light brightness were computed for a power-law spatial distribution of the form $n(r) \propto r^{-\nu}$, assuming that the scattering properties of the dust remain constant between 1 and 3.3 AU. Scattering functions typical of silicate particles (Gegenschein) and iron particles (no Gegenschein) were used at several elongations in addition to ϵ = 135-145 degrees. Since neither scattering functions nor the exact position of the spacecraft affected the relative brightness decrease, the shape of the curves in Figure 3 is not strongly dependent on the model parameters, provided that the scattering properties of the particles do not vary strongly with heliocentric distance.

The upper pair of curves in Figure 3 shows the effect of a dust cutoff at the outer edge of the asteroid belt on the predicted zodiacal light brightness. The solid line gives the predicted brightness for $\nu = 1.5$ and a dust distribution extended to infinity; in this case the brightness will vary as $I(R) \propto R^{-(\nu+1)}$. The dashed line represents the brightness variation for $\nu = 1.5$ at $r \leq 3.3$ AU and $n(r) = 0$ at $r > 3.3$ AU. The middle pair of curves compares $\nu = 1$ and $\nu = 2$, with a dust cutoff at 3.3 AU. From these examples and other, similar models, we conclude that a model with $\nu \approx 1$ and a cutoff near 3.3 AU gives the best fit to our observations for a single power-law distribution.

The lower curves give examples of the predicted brightness variation when an increased

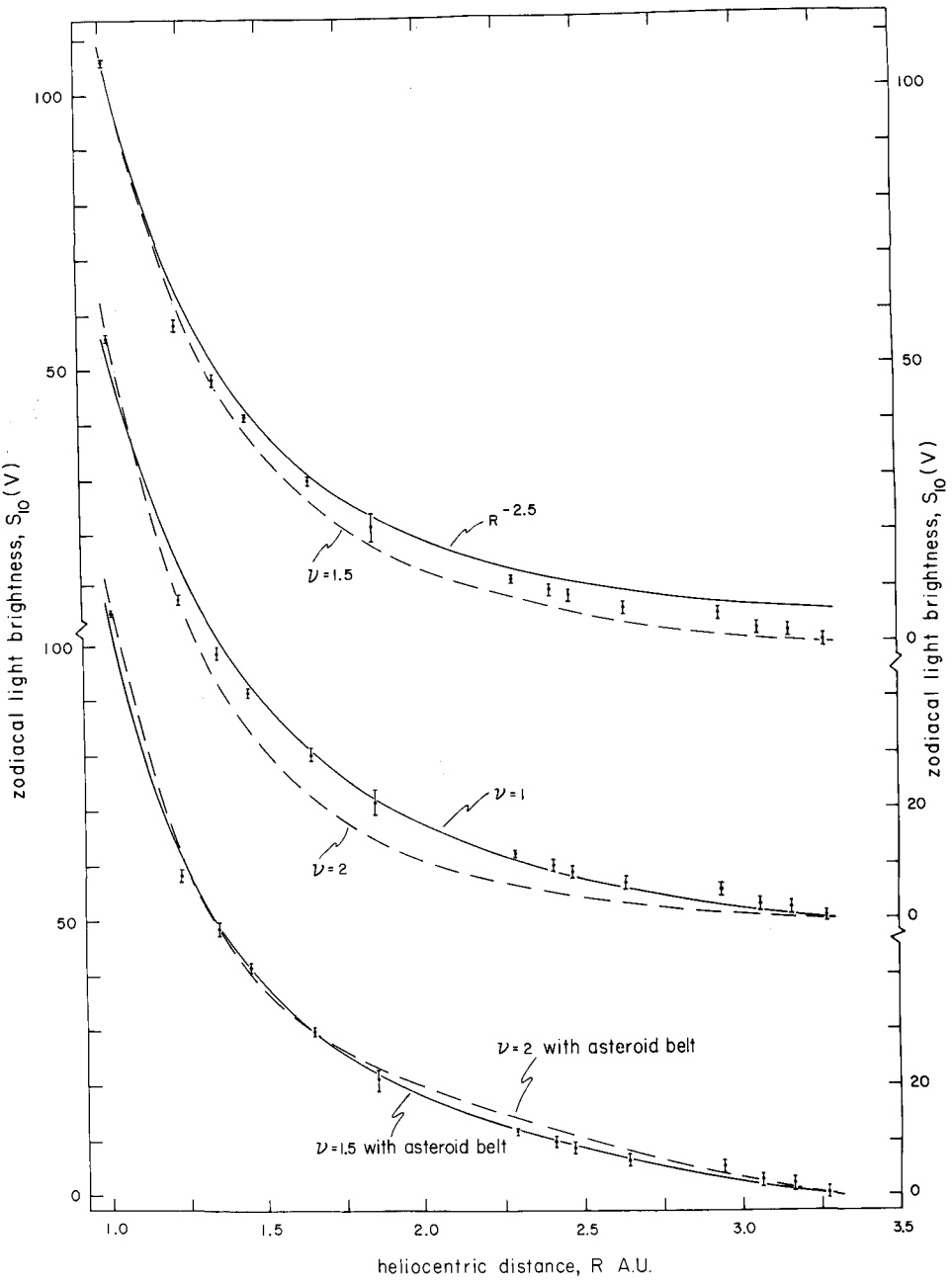

Fig. 3. Zodiacal light brightness vs. heliocentric distance. I = Pioneer 10 observations; ———, ------ are predicted models.

dust density in the asteroid belt is superimposed on a smooth power-law dust decrease. The composite dust distribution is of the form:

$$n(r) \propto n_0 r^{-\nu}, \qquad r < 2.3 \text{ AU}$$
$$n(r) \propto n_0 (r^{-\nu} + C), \qquad 2.3 \leq r \leq 3.3 \text{ AU}$$
$$n(r) = 0, \qquad r > 3.3 \text{ AU},$$

where n_0 is the interplanetary number density at 1 AU. The solid curve corresponds to $\nu = 1.5$, $C = 0.13$ and the dashed curve to $\nu = 2$, $C = 0.26$. Such a simplified 2-component model gives a particularly good fit for $\nu = 1.5$.

We conclude that, if the scattering properties of the dust particles (size, albedo) do not change significantly with heliocentric distance, then the spatial distribution can be satisfactorily represented by a smooth power law, $r^{-\nu}$, $\nu \approx 1$ or, equally well, by a 2-component model with $\nu \approx 1.5$ and increased dust in the asteroid belt. The observed brightnesses indicate a drop in the dust density near 3.3 AU, beyond which the zodiacal light is not detectable above the background starlight.

Acknowledgements. This research was supported by NASA contract NAS2-7963. Assistance was provided by Barbara Green, Helga Olender and Gary Toller.

References

Hanner, M. S. and C. Leinert, 1972, The Zodiacal Light as seen from the Pioneer F/G and Helios Probes, Space Research XII, 445-455.

Hanner, M. S. and J. L. Weinberg, 1973, Gegenschein Observations from Pioneer 10, Sky and Telescope, 45, 217-218.

Hanner, M. S. and J. L. Weinberg, 1974, Changes in Zodiacal Light with Heliocentric Distance: Preliminary Results from Pioneer 10, Space Research XIV, 769-771.

Hanner, M. S., J. L. Weinberg, L. M. DeShields II, B. A. Green, and G. N. Toller, 1974, Zodiacal Light and the Asteroid Belt: The View from Pioneer 10, J. Geophys. Res. 79, 3671-3675.

Hayes, D. S. and D. W. Latham, 1975, A Rediscussion of the Atmospheric Extinction and the Absolute Spectral Energy Distribution of Vega, Astrophys. J. 197, 593-601.

Johnson, F. S., 1954, The Solar Constant, J. Meteorol. 11, 431-439.

Labs, D. and H. Neckel, 1970, Transformation of the Absolute Solar Radiation Data into the International Practical Temperature Scale of 1968, Solar Phys. 15, 79-87.

Pellicori, S. F., E. E. Russell, and L. A. Watts, 1973, Pioneer Imaging Photopolarimeter Optical System, Appl. Opt. 12, 1246-1257.

Stebbins, J. and G. E. Kron, 1957, Six-Color Photometry of Stars. X. The Stellar Magnitude and Color Index of the Sun, Astrophys. J. 126, 266-280.

Weinberg, J. L., M. S. Hanner, H. M. Mann, P. B. Hutchison, and R. Fimmel, 1973, Observations of Zodiacal Light from the Pioneer 10 Asteroid-Jupiter Probe: Preliminary Results, Space Research XIII, 1187-1192.

Weinberg, J. L., M. S. Hanner, D. E. Beeson, L. M. DeShields II, and B. A. Green, 1974, Background Starlight Observed from Pioneer 10, J. Geophys. Res. 79, 3665-3670.